Application of the hidden-crossing method to positronium formation

S. J. Ward,[1] J. H. Macek,[2] and S. Yu. Ovchinnikov[2]
[1]*Department of Physics, University of North Texas, Denton, Texas 76203*
[2]*Department of Physics and Astronomy, University of Tennessee, Knoxville, Tennessee 37996 and Oak Ridge National Laboratory, P.O. Box 2009, Oak Ridge, Tennessee 37831*
(Received 3 August 1998)

We have applied the hidden-crossing method to compute *S*-, *P*-, and *D*-wave cross sections for Ps formation in positron-hydrogen collisions in the Ore gap. The hidden-crossing method has provided a physical explanation of why the *S*-wave cross section is so small and why the *D* wave is significant. The one-Sturmian theory is used to correct the hidden-crossing theory to take into account the factor $(\langle\varphi|d^2\varphi/dR^2\rangle+(1/4)/R^2)$. We have considered this correction term in computing the *P*- and *D*-wave cross sections. The hidden-crossing results are compared with accurate results from other methods. This comparison helps assess the accuracy of the hidden-crossing method in describing three-body collisions. [S1050-2947(99)06506-3]

PACS number(s): 34.85.+x, 34.70.+e, 36.10.Dr

I. INTRODUCTION

Positronium (Ps) formation in positron-hydrogen collisions probes the correlated motion of three charged particles. It is one of the simplest three-body processes that is now amenable to experimental investigation [1–4]. Positron collisions are of interest in astrophysics due to the observation of 511-keV γ rays from solar flares, from the galactic center [5,6], and very recently from above the galactic center [7]. Analysis of the width of the 511-keV line using accurate Ps-formation cross sections for positron-hydrogen collisions provides information on the ionization state and temperature of the radiating medium. The investigation of Ps formation provides ideas about chemical reactions in which the active positive particle has a very small mass [8]. The cross section for antihydrogen formation in antiproton-positronium collisions is related simply to the cross section for Ps formation in positron-hydrogen collisions [9]. This is because of charge conjugation and time reversal invariance. Antihydrogen is one of the most fundamental systems in physics and can be used to perform critical tests of CPT.

The Ps-formation cross section in positron-hydrogen collisions in the Ore gap has been accurately determined using a number of different methods. (The Ore gap is the energy region between the onset of Ps formation and the first excitation level of the target atom.) Benchmark *S*- and *P*-wave cross sections for Ps formation have been computed by Humberston and collaborators [10–14] using the Kohn variational method. The *D*-wave cross section [12,14,15] for Ps formation computed using the Kohn variational method converges more slowly with respect to the number of linear parameters than the *S* and *P* waves and is believed to be within 10% of the exact value. Extensive two-center close-coupling calculations have been performed, for instance, an 18-state calculation by McAlinden *et al.* [16] and Kernoghan *et al.* [17], a 33-state calculation by Kernoghan *et al.* [18], and 20, 21, and 28-state calculations by Mitroy and collaborators [19–21]. Gien [22] has employed the Harris-Nesbet method using a wave function that is comprised of the $1s$, $2s$, $2p$, and $3\overline{p}$ state of hydrogen and positronium together with algebraic Hylleraas correlation functions. His *D*-wave calculation for Ps formation is probably more accurate than the earlier Kohn variational calculations [14,22]. Igarashi and Toshima [23] and Zhou and Lin [24–26] have independently performed numerically elaborate hyperspherical close-coupling calculations for the first few partial waves. Even though the above methods determined accurately the partial wave cross sections for Ps formation in positron-hydrogen collisions in the Ore gap, a number of physical questions remained unanswered.

The hidden-crossing method is well adapted to elucidating underlying physical pictures [27]. We have applied the hidden-crossing method to Ps formation in positron-hydrogen collisions in the Ore gap and computed the *S*-, *P*-, and *D*-wave cross sections for Ps formation. It had been known for some time that the *S*-wave cross section was very small [10,11] and the *D*-wave is significant [15], but the reason was not known. Our calculation using the hidden-crossing method has provided the reason. We have reported our preliminary investigation of the application of this method to Ps formation in conference proceedings [28,29]. In Ref. [28] only the *S*-wave cross section was reported and in Ref. [29] the *P*- and *D*-wave cross sections reported were only preliminary. For the present paper we computed the eigenvalues for the *P* and *D* waves to a higher degree of accuracy than we did for Ref. [29]. In fact, in Ref. [29] we stated that the accuracy of the (*D*-wave) cross section with respect to the number of collocation points still needs to be determined. We have since determined the accuracy and it is stated in the present paper. A significant difference between Ref. [29] and the present paper is that in the present paper we demonstrate how the one-Sturmian theory is used to correct the hidden-crossing theory to take into account the factor $(\langle\varphi|d^2\varphi/dR^2\rangle+(1/4)/R^2)$. We consider this correction term in computing the *P*- and *D*-wave cross sections. Furthermore, in the present paper we derive the formulas used in Ref. [29] to take into account tunneling through the top of barrier (TOB).

It should be noted that Janev and Solov'ev [30] have recently reported the application of the hidden-crossing theory to positron-hydrogen collisions. Their hidden-crossing

method uses mass and charge transformations.

We used the hidden-crossing method formulated in the hyperspherical representation [27,31,32]. The significance of this formulation is that, unlike the conventional formulation, it does not employ a classical trajectory approximation and thus can be applied to the correlated motion of three charged particles of arbitrary mass and charge. For Ps formation, unlike charge exchange in ion-atom collisions, the relative motion between the projectile and target nucleus can never be treated classically. The hidden-crossing method successfully describes reactions in ion-atom collisions. Recently, the hidden-crossing method formulated in the hyperspherical representation has been shown to successfully describe electron-impact ionization [33,34]. Furthermore, experiments for positron-impact ionization of He and H_2 [35] can be interpreted by using the hidden-crossing method to extend the Wannier theory to higher energies [36]. Despite the success of the hidden-crossing method, it is not an exact method. Comparing our hidden-crossing results for Ps formation with results from other methods helps to assess the accuracy of the method in describing three-body Coulomb systems.

The hidden-crossing method formulated in the hyperspherical representation is outlined in Sec. II, numerical techniques are presented in Sec. III, results are given in Sec. IV, and the conclusion is provided in Sec. V. The model that we employed to describe tunneling through the TOB is given in Appendix A. The extension of the hidden-crossing method to include a correction term $(\langle\varphi|d^2\varphi/dR^2\rangle+(1/4)/R^2)$ is given in Appendix B. Atomic units are used throughout unless explicitly stated.

II. HIDDEN-CROSSING METHOD

The hidden-crossing method has its origins in the work of Landau [37] on transitions when the motion is quasiclassical. Using the hyperspherical representation, Macek and Ovchinnikov [27] and Macek [31,32] recently derived the hidden-crossing method without making any classical trajectory approximations. Their derivation of the hidden-crossing method begins with an integral transform, known as the Kontorovich-Lebedeev transform [38], and an expansion in angle-Sturmian functions. Approximating the expansion by a single angle-Sturmian function and evaluating the integral form of the wave function at large hyper-radius using the stationary phase approximation leads to the hidden-crossing method. Since this derivation of the hidden-crossing method has been presented in detail elsewhere [27,31,32] we give only a brief review below. Hyperspherical coordinates and adiabatic bases are described in Sec. II A. The angle-Sturmian basis functions are defined in Sec. II B. The Kontorovich-Lebedeev transform and the approximations made to derive the hidden-crossing method are presented in Sec. II C.

A. Hyperspherical coordinates and basis functions

Hyperspherical coordinates were first introduced in atomic physics by Gronwall in 1932 [39] to study the analytic structure of the Schrödinger equation for ground-state helium. However, hyperspherical coordinates with adiabatic bases were first introduced by Macek in 1968 [40] to study doubly excited states of helium. Zhou and Lin [24] presented hyperspherical coordinates corresponding to three sets of Jacobi coordinates for the positron-hydrogen system. We used their α set and made the approximation that the proton is infinitely massive. In the α set the hyper-radius R is defined as $\sqrt{r_1^2+r_2^2}$, the tangent of hyperangle α as r_2/r_1, where $\mathbf{r}_1$ and $\mathbf{r}_2$ are the position vectors of the positron and electron with respect to the proton, respectively. As is usual in the hyperspherical treatment the reduced wave function $\Psi(R,\Omega)$ is written in terms of the standard wave function $\psi(R,\Omega)$ $[\Psi(R,\Omega)=R^{5/2}(\sin\alpha)(\cos\alpha)\psi(R,\Omega)]$ so the Schrödinger equation becomes [24]

$$\left[-\frac{\partial^2}{\partial R^2}+\frac{\Lambda^2+2RC(\Omega)}{R^2}-2E\right]\Psi=0, \tag{1}$$

where Ω represents five hyperangles and Λ^2 is the grand angular momentum operator as given by Zhou and Lin [24]. The scaled potential $C(\Omega)$ in Eq. (1) is just the product of the hyperradius R and the Coulomb interaction between the charged particles. The hyperspherical adiabatic basis functions $\varphi(R,\Omega)$ are defined as eigenfunctions of the operator $[\Lambda^2+\frac{1}{4}+2RC(\Omega)]$ where R is held fixed, i.e.,

$$[\Lambda^2+\tfrac{1}{4}+2RC(\Omega)]\varphi(R;\Omega)=2\varepsilon'_\mu(R)R^2\varphi(R;\Omega). \tag{2}$$

In Eq. (2), $\varepsilon_\mu(R)=\varepsilon'_\mu(R)-\frac{1}{2}(1/4R^2)$ are the adiabatic energy eigenvalues.

B. Angle-Sturmian bases

The adiabatic hyperspherical basis functions are obtained by holding R fixed and using $\varepsilon'(R)$ as the eigenvalue. An alternative basis, the angle-Sturmian basis functions $S_n(\nu,\Omega)$, are obtained by holding $\varepsilon'(R)R^2$ fixed and using the coefficient of the scaled potential $C(\Omega)$, $\rho_n(\nu)$ as the eigenvalue;

$$[\Lambda^2+2\rho_n(\nu)C(\Omega)]S_n(\nu;\Omega)=(\nu^2-1/4)S_n(\nu;\Omega). \tag{3}$$

The quantity $\nu^2-1/4$ is held fixed and $\rho_n(\nu)$ is adjusted so that the boundary conditions on $S(\nu;\Omega)$ are satisfied. The orthogonality condition of the Sturmian basis functions is

$$-2\int S_n(\nu;\Omega)C(\Omega)S_{n'}(\nu;\Omega)d\Omega=\delta_{n,n'}. \tag{4}$$

The angle-Sturmian basis relates to the hyperspherical adiabatic basis according to Demkov's construction [41]. This construction considers that the adiabatic eigenvalues $\varepsilon_\mu(R)$ correspond to different branches of the same function $\varepsilon(R)$, which is single valued on a multisheeted Riemann surface. Surfaces corresponding to different eigenvalues are connected at branch points. Near a branch point R_b the energy function $\varepsilon(R)$ has the form $\varepsilon(R)\approx\sqrt{R-R_b}$, i.e., the branch points are square-root branch points. The appropriate Riemann surface can be constructed by plotting $\mathrm{Re}[\varepsilon(R)]$ vs R. The surface defines a single function $\varepsilon(R)$ for all R. The standard hyperspherical adiabatic eigenfunctions are different branches of this function for real values of R. The equation,

$$2\varepsilon(\rho)\rho^2=\nu^2-\tfrac{1}{4}, \tag{5}$$

may be solved to find the roots $\rho_n(\nu)$, which are the Sturmian eigenvalues Eq. (3). The corresponding Sturmian eigenfunctions $S_n(\nu;\Omega)$ are, aside from normalization constants, just the adiabatic functions $\varphi(R;\Omega)$ evaluated at $R=\rho_n(\nu)$:

$$S_n(\nu;\Omega)=N(\nu)\varphi(\rho_n(\nu);\Omega). \tag{6}$$

The normalization $N(\nu)$ can be determined from the orthogonality condition Eq. (4) and is given by Ref. [27],

$$N(\nu)=\sqrt{-\frac{\partial\rho_n(\nu)}{2\nu\partial\nu}}. \tag{7}$$

C. Kontorovitch-Lebedeev transform

Any arbitrary function of R can be expressed in terms of Bessel functions $Z_\nu(KR)$ of fixed energy $E=K^2/2$. This is the Kontorovitch-Lebedeev transform [38] and it is given by

$$\Psi(R;\Omega)=\int_c 2\nu d\nu R^{1/2}Z_\nu(KR)\Phi(\nu,\Omega), \tag{8}$$

where c denotes a contour in the ν plane that depends upon boundary conditions. This transform is analogous to the Fourier transform in the time-dependent representation. For particles interacting via Coulomb interactions, the Schrödinger equation is not separable in hyperspherical coordinates. Therefore, the coefficient $\Phi(\nu;\Omega)$ is expanded in angle-Sturmian bases. The simplest approximation to make is to truncate the expansion to one-term. A closed-form expression to the wave function for the one-Sturmian approximation is given by Macek and Ovchinnikov [27] and Macek [31,32].

The hidden-crossing method emerges by considering the asymptotic form ($R\to\infty$) of the one-Sturmian wave function and evaluating the integral using the stationary phase approximation. The resulting wave function, aside from an unimportant overall multiplicative constant, is given by

$$\Psi(R,\Omega)\approx\sum_{\text{paths}}\sum_{\mu}\frac{1}{\sqrt{K_\mu(R)}} \times\exp\left(i\int_{c_{n\mu}}^{R}K_\mu(R')dR'\right)\varphi_\mu(R;\Omega),\quad R\to\infty. \tag{9}$$

In Eq. (9) $c_{n\mu}$ denotes a contour that connects $\varphi_a(R_0;\Omega)$ at small R_0 with $\varphi_\mu(R;\Omega)$ at large R and the sum over paths goes over all such contours. The value R_0 is a relatively small value of R corresponding to $K_a(R_0)=0$, and a represents an adiabatic label that may differ from the label μ appropriate at large R. The label a specifies the branch of the function $\varepsilon(R)$ at small R. The wave-vector $K_\mu(R)$ is defined according to

$$K_\mu^2(R)=K^2-\frac{\nu_\mu^2}{\rho(\nu_\mu)^2}=K^2-\frac{\nu_\mu^2}{R^2}=K^2-2\varepsilon_\mu(R)-\frac{1/4}{R^2} =K^2-2\varepsilon'_\mu(R). \tag{10}$$

Note that Eq. (9) is of WKB form and that Eq. (10) involves the Langer correction $(1/4)/R^2$. From the asymptotic wave function Eq. (9) the Jost function [42] may be extracted. The S matrix computed by forming $\Sigma_a[(J^-)^{-1}]_{ia}J^+_{a\mu}$ is equivalent to the standard hidden-crossing expression [37].

The S-matrix element S_{12} for Ps formation in the Ore gap is obtained by forming

$$S_{12}=\sum_{a=1}^{2}[(J^-)^{-1}]_{1,a}J^+_{a,2}. \tag{11}$$

The first term ($a=1$) of this sum is given by integrating inward from a point R_i on the first sheet of the Riemann surface [the e^+-H($1s$) sheet] to the classical turning point R_1^t using the negative branch of the wave-vector $K_1(R)$, then outward using the positive branch of $K_1(R)$, going clockwise around the branch point R_b to get to a point R_f on the second sheet [the $p+\text{Ps}(1s)$ sheet]. The second term ($a=2$) corresponds to integrating inward from R_i using the negative branch of K_1, going counterclockwise around the branch point to the turning point of the second sheet R_2^t, and outward using the positive branch of K_2 to the point R_f. The Ps-formation matrix element S_{12} is the *coherent* sum of the contribution corresponding to the two paths.

The modulus square of the S-matrix element $|S_{12}|^2$ can be expressed in the form,

$$|S_{12}|^2=4P\sin^2\Delta_{12}, \tag{12}$$

where the probability P is given by

$$P=\exp\left[-2\left|\text{Im}\int_c K(R)\,dR\right|\right], \tag{13}$$

and the phase Δ_{12} by

$$\Delta_{12}=\left|\text{Re}\int_c K(R)\,dR\right|. \tag{14}$$

The contour c is from R_1^t, around R_b, to R_2^t. As is standard procedure in computing $|S_{12}|^2$, we multiply the right-hand side of Eq. (12) by $1-P$. The $1-P$ term comes from the unitary of the Jost matrix and its justification can be found in a number of places, for instance, Nikitin and Umanskii [43]. Finally, the partial-wave (L) cross section in units of πa_o^2 for Ps formation in the Ore gap is given by

$$\sigma_{12}^{(L)}=\frac{2L+1}{2E+1}|S_{12}|^2. \tag{15}$$

III. NUMERICAL TECHNIQUES

Following the treatment of Zhou and Lin [24], we diagonalized the operator $[\Lambda^2+\frac{1}{4}+2RC(\Omega)]$ by writing the eigenfunctions $\varphi(R;\Omega)$ in terms of the Euler angles. This diagonalization leads to coupled partial differential equations in terms of the variables α and θ_{12} [24,34], where $\cos\theta_{12}=\hat{\mathbf{r}}_1\cdot\hat{\mathbf{r}}_2$. We solved these equations to compute the eigenvalues $\varepsilon'_\mu(R)$ using the basis-spline collocation method (BSCM) [44–47]. This method employs polynomials of order N on an interval in the range of a coordinate. We used the

TABLE I. S-wave cross section in units of πa_o^2 for Ps formation in the Ore gap.

k_i (a.u)	0.71	0.75	0.80	0.85
Hidden crossing	0.00031	0.00041	0.00045	0.00047
Hidden crossing without the Langer correction	0.0042	0.0055	0.0062	0.0066
Kohn variational [10–12,14,15]	0.0041	0.0044	0.0049	0.0057
Harris-Nesbet [22]	0.00405	0.00426	0.00479	0.00552
21-state CC($\overline{13,8}$) [20]	0.00405	0.00427	0.00472	0.00560
Hyperspherical [23]	0.00404	0.00398	0.00462	0.00535
Hyperspherical [24,25]	0.00397	0.00427	0.00483	0.00557

BSCM codes developed by Bottcher and co-workers [44–46] and Kegley Jr. *et al.* [47] and to diagonalize the complex non-Hermitian matrix a routine from LAPACK, CGEEV [48]. The order of the matrix that we diagonalized is given by the product n_α, n_θ, and $L+1$, where n_α (n_θ) is the number of collocation points for the α (θ) coordinate, and L is the total orbital angular momentum of the system.

For the S-wave calculation we used fifth-order polynomials for each interval in the range of the α coordinate and the θ_{12} coordinate. We optimized the distribution of α collocation points at $R=3$ and 4.4 a.u. A uniform distribution of collocation points was used for the θ_{12} coordinate. We used 32 collocation points for α, 30 collocation points for θ_{12}, and a mesh spacing of 0.025 a.u. The S-wave cross section has converged to within 2% with respect to the number of collocation points, and to within 9% with respect to the number of integration points.

To compute the P-wave eigenvalues around the branch point (R_b) and along the real axis to the left of the real part of the branch point [Re(R_b)] we used 28 collocation points for both α and θ_{12} coordinates. However, along the real axis to the right of the real part of the branch point [Re(R_b)] we used 38 collocation points for α and 34 collocation points for θ_{12}. We used a mesh spacing of 0.05 a.u. for the integration. For the α coordinate we used fifth-order polynomials and a nonuniform distribution of collocation points.

To determine accurately the eigenvalues out even to large R, which is needed for the investigation of the near-threshold behavior, we computed the eigenvalues using different order polynomials and distribution of collocation points for θ_{12}. In the first calculation we used for the coordinate θ_{12} fifth-order polynomials and a linear distribution of collocation points. In the second calculation in the computation of the eigenvalues around R_b and to the left of Re(R_b) we again used for the coordinate θ_{12} fifth-order polynomials and linear distribution of collocation points. However, in the computation of the eigenvalues to the right of Re(R_b), we used for θ_{12} third-order polynomials and a quadratic distribution of collocation points starting from the origin. The P-wave cross section computed using the eigenvalues obtained in the two calculations differs by less than 3%, 0.9%, and 0.06% at $k_i=0.75$, 0.80, and 0.85 a.u., respectively. The convergence tests that we give below and the results that we present in Sec. IV B corresponds to the second calculation.

The convergence of the P-wave cross section with respect to the number of integration points is 0.4%, 0.4%, and 0.1% at $k_i=0.75$, 0.80, and 0.85 a.u., respectively. The P-wave cross section appears to have converged to within 5% with respect to the number of collocation points.

We used the same number of collocation points to compute the D-wave eigenvalues as we used to compute the P-wave eigenvalues. We used fifth-order polynomials for the α and θ_{12} coordinates, and a mesh spacing of 0.05 a.u. for the integration.

To test the sensitivity of the cross section on the order of polynomial and distribution of collocation points for θ_{12}, for a given set of collocation points, we performed two sets of calculations. In the first calculation we used for the θ_{12} coordinate fifth-order polynomials and a linear distribution of collocation points. In the second calculation in the computation of the eigenvalues around R_b and to the left of Re(R_b) we again used for the θ_{12} coordinate fifth-order polynomials and linear distribution of collocation points. However, in the computation of the eigenvalues to the right of Re(R_b), we used for θ_{12} third-order polynomials and a quadratic distribution of collocation points starting from the origin. The D-wave cross section computed using the eigenvalues obtained in the two calculations differs by less than 14%, 4%, and 2% at $k_i=0.75$, 0.80, and 0.85 a.u., respectively. The convergence tests that we give below and the results that we present in Sec. IV C corresponds to the first calculation.

The D wave has converged to within 0.07% with respect to the number of integration points. The convergence with respect to the number of collocation points improves considerably with increasing energy. For instance, the convergence is about 11%, 3%, and 2% at $k_i=0.75$, 0.80, and 0.85 a.u., respectively.

IV. RESULTS

A. S wave

The phase Δ_{12}, Eq. (14), for S-wave scattering is close to π ($\Delta_{12}\sim 3.2$ rad). Thus, there is almost complete destructive interference between the two amplitudes [paths $a=1$ and 2 of Eq. (11)] that correspond to different paths leading to Ps formation. Hence, the S-wave cross section is very small and highly sensitive to the accuracy with which the phase is determined. We give the S-wave cross section for Ps formation within the Ore gap in Table I and compare it with the Kohn variational [10–12,14], the Harris-Nesbet [22], the 21-state close-coupling CC($\overline{13,8}$) [20], and the hyperspherical [23–25] calculations. In Table I we also show the cross section computed by adding an *ad hoc* factor $(1/4)/R^2$ to the

TABLE II. P-wave cross section in units of πa_o^2 for Ps formation in the Ore gap.

k_i (a.u)	0.75	0.80	0.85
Hidden crossing	0.381	0.558	0.696
Hidden crossing with correction term $(\langle\varphi\|d^2\varphi/dR^2\rangle+(1/4)/R^2)$	0.327	0.510	0.679
Kohn variational [12–15]	0.3657	0.4819	0.5627
Harris-Nesbet [22]	0.366	0.483	0.564
21-state CC$(\overline{13,8})$ [20]	0.366	0.483	0.563
Hyperspherical [23]	0.376	0.490	0.570

right-hand side of Eq. (10) which means neglecting the Langer correction. We refer to this calculation as hidden crossing without the Langer correction. Even though this factor is *ad hoc*, it shows the factor required to obtain a cross section in reasonable agreement with the Kohn variational results. It also shows the extreme sensitivity of the S-wave cross section to a small change in the phase—a change of 2.7–2.8% in the phase causes the cross section to increase by a factor 13–14. The calculation of the S-wave cross section has thus provided an extremely sensitive test of the hidden-crossing method. Interestingly, for $k_i=0.71$, 0.75, and 0.80 a.u., the classical turning point of the second sheet (R_2^t) is at a larger R value than the real part of the branch point $[\mathrm{Re}(R_b)]$. Thus, for these values of the incident wave-vector Ps formation for the S wave occurs via tunneling.

B. P wave

We present the P wave hidden-crossing cross section for Ps formation in Table II, and compare it with the Kohn variational [12–15], the Harris-Nesbet [22], the 21-state close coupling CC$(\overline{13,8})$ [20], and the hyperspherical [23] cross sections. In Fig. 1 we compare the hidden-crossing results with the Kohn variational [12–15,49] and Harris-Nesbet [22] results. The hidden-crossing results agree with the Kohn variational results [12–15] to within 5%, 16%, and 33% at $k_i=0.75$, 0.80, and 0.85 a.u., respectively. We are

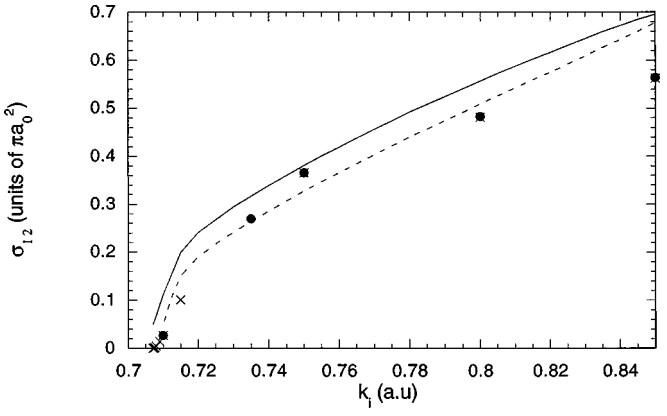

FIG. 1. P-wave cross section for Ps formation for positron-hydrogen collisions in the Ore gap. The hidden-crossing results are represented by the solid curve whereas the hidden crossing with the correction term $(\langle\varphi|d^2\varphi/dR^2\rangle+(1/4)/R^2)$ results are represented by the dashed curve. The Kohn variational results [12–15,49] and Harris-Nesbet results [22] are represented, respectively, by crosses and solid dots.

presently unclear why there is such a discrepancy at $k_i=0.85$ a.u., but we note that the classical turning point of the second sheet R_2^t is very close to the real part of $\mathrm{Re}(R_b)$, within 0.05 a.u. For P-wave scattering, Ps formation occurs via tunneling for the entire Ore gap and the phase is close to 2.3 rad.

Near-threshold Ps formation is of current interest [14,50]. As one decreases the energy of the incoming positron, the classical turning point for the second sheet (R_2^t) moves out to larger real R. The behavior of the second eigenvalue $\varepsilon_2'(R)$ at large real R is similar in shape to the potential shown in Fig. 3 of Ref. [51] up to $x=x_3$. The eigenvalue $\varepsilon_2'(R)$ decreases with increasing R to a minimum at $R=9.9$ a.u., increases to a maximum at $R=15.05$ a.u., and then decreases again. The value of the maximum of $\varepsilon_2'(R)$ is -0.2488 a.u. $(k_i=0.7088$ a.u.). This means that for wave numbers up to $k_i=0.7088$ a.u. there occurs in addition to the classical turning point (R_2^t) two other classical turning points, $R_{2,\mathrm{TOB},1}^t$ and $R_{2,\mathrm{TOB},2}^t$. Thus, the eigenvalue $\varepsilon_2'(R)$ curve has a TOB region. The effect of the TOB is most significant on the cross section near threshold. In considering tunneling through the TOB we apply the analysis of Macek and Ovchinnikov [51] to Ps formation. We present this application in Appendix A. The cross section that takes into account tunneling through the TOB region is given by

$$\sigma_{12}^{(L)}=|\mathcal{T}|^2\sigma_{12}^{(L)}(R_2^t), \tag{16}$$

where $\sigma_{12}^{(L)}(R_2^t)$ is the cross section computed by integrating $K(R)$ along a contour that starts from R_1^t, goes around the branch point R_b to R_2^t, and $|\mathcal{T}|^2$ is the modulus squared of the transmission coefficient given in Appendix A. Figure 1 shows that the P-wave cross section for Ps formation computed using Eq. (16) rises fairly rapidly up to $k_i=0.715$ a.u.

In Appendix B we show that the one-Sturmian theory [27] can be used to correct the hidden-crossing method to take into account the correction term $(\langle\varphi|d^2\varphi/dR^2\rangle+(1/4)/R^2)$. The factor $\varepsilon_\mu(R)+W_\mu(R)$, where $W_\mu(R)=-\frac{1}{2}\langle\varphi|d^2\varphi/dR^2\rangle$, gives the close-coupling asymptotic channel potentials through terms of order $1/R^2$ [40,52,53]. Using the one-Sturmian theory it can be shown that for large R, where $\varepsilon(R)$ is a slowly varying function of R the wave vector

$$K_\mu^2(R)=K^2-2\varepsilon_\mu(R)-2W_\mu(R) \tag{17}$$

with the neglect of terms of order $1/R^4$. The asymptotic form of the second derivative term $\langle\varphi_2|d^2\varphi_2/dR^2\rangle$ for the p-Ps(1s) channel is given by [53]

TABLE III. D-wave cross section in units of πa_o^2 for Ps formation in the Ore gap.

k_i (a.u)	0.75	0.80	0.85
Hidden crossing	0.322	0.816	1.205
Kohn variational [12,14,15]	0.312	0.820	1.083
Harris-Nesbet [22]	0.321	0.860	1.158
21-state CC($\overline{13,8}$) [20]	0.320	0.859	1.158
Hyperspherical [23]	0.334	0.866	1.16

$$\left\langle \varphi_2 \left| \frac{d^2\varphi_2}{dR^2} \right\rangle \sim -\frac{3}{4R^2} \quad \text{as} \quad R\to\infty \tag{18}$$

with the neglect of terms of order $1/R^4$. Since Eq. (17) is valid for large R, we used Eq. (17) with Eq. (18) in integrating $K_2(R)$ along the real axis to the right of $\mathrm{Re}(R_b)$. For other values of R in the contour of $\int_c K(R)\,dR$, i.e., around R_b and to the left of $\mathrm{Re}(R_b)$, we used $K_\mu(R)$ defined according to Eq. (10). There occurs a very slight TOB in the term $\varepsilon_2(R)+W_2(R)$ at large R. This term decreases with increasing R to a minimum of -0.2477 ($k_i=0.7104$ a.u.) at $R=10.85$ a.u., increases to a maximum of -0.2476 a.u. ($k_i=0.71055$ a.u.) at $R=13.05$ a.u., and then decreases again. As before, we approximated the TOB region by an inverted harmonic oscillator. For k_i greater than 0.7104 a.u. we computed the cross section according to Eq. (16). This cross section is given in Table II and Fig. 1. We refer to this cross section as the hidden crossing with the correction $(\langle\varphi|d^2\varphi/dR^2\rangle+(1/4)/R^2)$ since we have used Eq. (17). The agreement of this cross section with the Kohn variational results is 11%, 6%, and 21% at $k_i=0.75$, 0.80, and 0.85 a.u., respectively. The correction term enables better agreement to be achieved with the Kohn variational results at $k_i=0.80$ and 0.85 a.u.

C. D wave

The phase Δ_{12}, Eq. (14), for the D wave is close to $\pi/2$ ($\Delta_{12}\approx 1.66\to 1.61$ rad for $k_i=0.75\to 0.85$ a.u.). Thus, unlike S-wave scattering where there is almost complete destructive interference between the two amplitudes [paths $a=1$ and 2 of Eq. (11)] corresponding to different paths that lead to Ps formation, for the D wave there is close to constructive interference between the two amplitudes. Thus, the hidden-crossing method has provided an explanation of why the D-wave contribution to the Ps-formation cross section in the Ore gap is so significant. We did not observe a TOB region in the second eigenvalue for the D wave. In Table III we compare the hidden-crossing cross section with the Kohn variational [12,14,15,20,23], the Harris-Nesbet [22], the 21-state close-coupling CC($\overline{13,8}$) [17], and the hyperspherical [20] cross sections. The hidden-crossing results agree with the Kohn variational results to within 3%, 0.5%, and 11% at $k_i=0.75$, 0.80, and 0.85 a.u., respectively. However, Humberston *et al.* [14] explain that their D-wave cross section is less well converged than their S- and P-wave cross section, and that the Harris-Nesbet calculation of the D wave is probably more accurate than their Kohn variational calculation. Our hidden-crossing results agree with the Harris-Nesbet results to within 0.3%, 5%, and 4% at $k_i=0.75$, 0.80, and 0.85 a.u., respectively. For $k_i=0.80$ and 0.85 a.u., the agreement between the Kohn variational and the hidden-crossing results is better for the D wave than the P wave. We note that the centrifugal barrier is larger for the D-wave than for the P wave. This causes the classical turning points to be at larger values of R for the D wave than they are for the P wave. The classical turning point for the second sheet R_2^t is further from the branch point for the D wave than the P wave. Furthermore, since the phase Δ_{12} for the D wave is close to $\pi/2$, the cross section is fairly insensitive to slight changes in the phase. For instance, at $k_i=0.85$ a.u., the phase Δ_{12} equals 1.609 rad. A change of 1% of this phase changes the cross section by less than 0.15%. We also computed the D-wave cross section by allowing for the correction term to the hidden-crossing method, $(\langle\varphi|d^2\varphi/dR^2\rangle+(1/4)/R^2)$, in the manner explained in Sec. IV B and Appendix B. This cross section is compared in Fig. 2 with the hidden crossing without the correction term, the Kohn variational [14,49], and the Harris-Nesbet [22] results. The effect of the correction term is to lower the cross section.

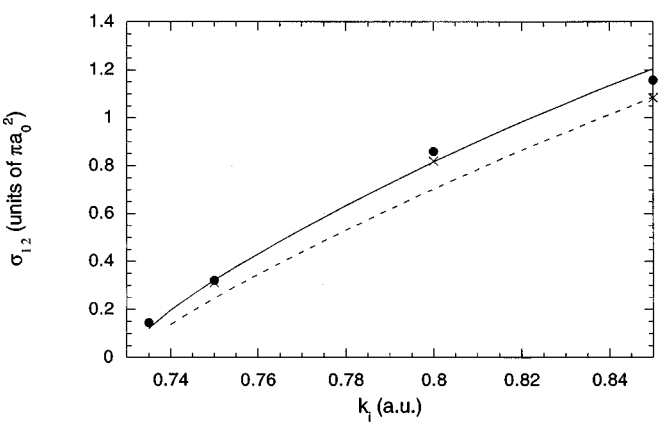

FIG. 2. D-wave cross section for Ps formation for positron-hydrogen collisions in the Ore gap. The hidden-crossing results are represented by the solid curve whereas the hidden crossing with the correction term $(\langle\varphi|d^2\varphi/dR^2\rangle+(1/4)/R^2)$ results are represented by the dashed curve. The Kohn variational results [12,14,15,49] and Harris-Nesbet results [22] are represented, respectively, by crosses and solid dots.

V. CONCLUSION

Using the hidden-crossing method formulated in the hyperspherical representation we have computed the S-, P-, and D-wave cross section for Ps formation in positron-hydrogen collisions in the Ore gap. The agreement of the P- and D-wave hidden-crossing results with the Kohn variational [12–15,49] and the Harris-Nesbet [22] results is fair to good. The hidden-crossing method has provided a physical explanation of why the S-wave cross section is very small and the D-wave is significant. The explanation is that for S-wave scattering there occurs almost complete destructive interference between the two amplitudes that correspond to different paths leading to Ps formation whereas for the D wave the two amplitudes almost completely constructively interfere.

For the P wave there occurs a TOB in the second eigenvalue at large R. We investigated the effect of tunneling

through the TOB region. We have shown that the one-Sturmian theory can be used to correct the hidden-crossing method to take into account the factor $(\langle\varphi|d^2\varphi/dR^2\rangle + (1/4)/R^2)$. We considered the correction term in computing the *P*- and *D*-wave cross sections for Ps formation.

ACKNOWLEDGMENTS

We appreciate communications with Dr. J. W. Humberston, Dr. T. T. Gien, Dr. C. D. Lin, Dr. P. Van Reeth, and Dr. Y. Zhou. We thank Dr. J. W. Humberston and Dr. P. Van Reeth for providing us with tables of their *S*-, *P*-, and *D*-wave cross sections for Ps formation. We also thank Dr. Y. Zhou and Dr. C. D. Lin for providing us with their tables of computed adiabatic potentials for the positron-hydrogen system, which we used for comparison purposes. S. J. W. gratefully acknowledges prior support by the National Science Foundation under Grant No. PHY-9213900, and UNT faculty research grants. J. H. M. gratefully acknowledges support by the National Science Foundation under Grant No. PHY-9222489 and travel support under NATO Grant No. CRG-950407. S. J. W. and J. H. M. both acknowledge support from the Institute for Theoretical Atomic and Molecular Physics at the Harvard-Smithsonian for Astrophysics where some of this work was undertaken. Oak Ridge National Laboratory is managed by Lockheed Martin Energy Research Corporation under Contract No. DE-AC05-96OR22464 with the U.S. DOE.

APPENDIX A: TUNNELING THROUGH TOB

The behavior of the second eigenvalue $\varepsilon_2'(R)$ is interesting in that there is a TOB region at large R. The shape of $\varepsilon_2'(R)$ as a function of R, at large R, is similar to that of Fig. 3 of Ref. [51] up to $x=x_3$. We apply the analysis of Ref. [51] in our treatment of the TOB region.

Without the TOB region, the wave function for $R>R_2^t$ is of the form,

$$\psi = S_{12}^{(0)} e^{i\int_{R_2^t}^{R} K_2(R')\,dR'}, \tag{A1}$$

where the *S*-matrix element $S_{12}^{(0)}$ is the amplitude of the outgoing radial wave in the absence of the TOB region. [Note, in writing Eqs. (A1)–(A3) and Eq. (A9) we did not include the normalization factor $1/\sqrt{K(R)}$ that multiplies the right-hand side of these equations. Furthermore, we neglected in Eqs. (A6), (A8), and (A9) phase factors that can be incorporated into the definition of the transmission $\mathcal{T}$ and reflection $\mathcal{R}$ coefficients.]

Now let us consider the TOB region, $R_{2,TOB,1}^t \leqslant R \leqslant R_{2,TOB,2}^t$, which is region III of Fig. 3 of Ref. [51]. Within the TOB region reflection and transmission occurs at the boundaries for both $E<\varepsilon_2'(R_T)$ and $E>\varepsilon_2'(R_T)$. To the left of the TOB region, $R_2^t<R\leqslant R_{2,TOB,1}^t$, i.e., region II of Fig. 3 of Ref. [51], the form of the wave function is a linear combination of an incident and reflected wave,

$$\psi_{II} = S_{12}^{(0)}[e^{i\int_{R_2^t}^{R} K_2(R')\,dR'} + B_r e^{-i\int_{R_2^t}^{R} K_2(R')\,dR'}], \tag{A2}$$

where B_r is a reflection coefficient. However, to the right of the TOB region, $R_{2,TOB,2}^t \leqslant R < R \to \infty$, the wave function is an outgoing wave,

$$\psi_{IV} = S_{12}^{(0)} \mathcal{T} e^{i\int_{R_{2,TOB,2}^t}^{R} K_2(R')\,dR'}, \tag{A3}$$

where $\mathcal{T}$ is the transmission coefficient.

In the TOB region, following the analysis of Ref. [51] we approximate $\varepsilon_2'(R)$ by an inverted harmonic oscillator,

$$\varepsilon_2'(R) = \varepsilon_2'(R_T) + \tfrac{1}{2}[\varepsilon_2'(R_T)]''(R-R_T)^2, \tag{A4}$$

where R_T is the TOB position, $\varepsilon_2'(R_T)$ is the eigenvalue at this position, and $[\varepsilon_2'(R_T)]''<0$.

The solutions of

$$\left[-\frac{d^2}{dR^2} + 2\varepsilon_\mu'(R) - K^2\right]\psi = 0 \tag{A5}$$

in the TOB region, region III, are parabolic functions. The wave functions in regions II, III, and IV need to be matched. We follow the treatment of Ref. [51] in recognizing that to match the solutions in regions II and III, the solution in region III is written in the form,

$$\psi_{III} = S_{12}^{(0)}[E^*(a,-(R-R_T)\gamma) + \mathcal{R}E(a,-(R-R_T)\gamma)], \tag{A6}$$

where

$$a = -\frac{E-\varepsilon_2'(R_T)}{\{-[\varepsilon_2'(R_T)]''\}^{1/2}}, \tag{A7}$$

$\gamma^4 = -4[\varepsilon_2'(R_T)]''$, and $\mathcal{R}$ is the reflection coefficient to be determined. To determine $\mathcal{R}$ and $\mathcal{T}$ Eq. (A6) needs to be expressed in the form of ingoing and outgoing waves. We use Eq. (19.18.3) of Ref. [54] to write Eq. (A6) in the form,

$$\begin{aligned}\psi_{III} = S_{12}^{(0)}\Bigg\{&\frac{1}{i}[\sqrt{1+e^{2\pi a}}E(a,(R-R_T)\gamma) \\ &- e^{\pi a}E(a,(R-R_T)\gamma)] + \mathcal{R}\left(-\frac{1}{i}\right)[\sqrt{1+e^{2\pi a}} \\ &\times E^*(a,(R-R_T)\gamma) - e^{\pi a}E(a,(R-R_T)\gamma)]\Bigg\}.\end{aligned} \tag{A8}$$

Furthermore, using Eq. (3.8) of Ref. [51] gives

$$\begin{aligned}\psi_{III} = \frac{S_{12}^{(0)}}{i}\{&-[e^{\pi a} + \mathcal{R}\sqrt{1+e^{2\pi a}}]e^{-i\int_{R_{2,\mathrm{TOB},2}^t}^{R} K_2(R')\,dR'} \\ &+ [\sqrt{1+e^{2\pi a}} + \mathcal{R}e^{\pi a}]e^{i\int_{R_{2,\mathrm{TOB},2}^t}^{R} K_2(R')\,dR'}\}.\end{aligned} \tag{A9}$$

Matching the wave function in region III, Eq. (A9) with the outgoing wave in region IV, Eq. (A3) gives

$$\begin{aligned} e^{\pi a} + \mathcal{R}\sqrt{1+e^{2\pi a}} &= 0, \\ \sqrt{1+e^{2\pi a}} + \mathcal{R}e^{\pi a} &= \mathcal{T}. \end{aligned} \tag{A10}$$

Thus, the modulus square of $\mathcal{R}$ and $\mathcal{T}$ are given, respectively, by

$$|\mathcal{R}|^2=\frac{e^{2\pi a}}{1+e^{2\pi a}},$$

$$|\mathcal{T}|^2=\frac{1}{1+e^{2\pi a}}. \tag{A11}$$

Since the coefficient of the outgoing wave in region IV is S_{12}, which equals $S_{12}^{(0)}\mathcal{T}$, the Ps-formation cross section that takes into account the TOB region is given by

$$\sigma_{12}^{(L)}=\frac{2L+1}{2E+1}|S_{12}|^2=|\mathcal{T}|^2\sigma_{12}^{(L)}(R_2^t), \tag{A12}$$

where

$$\sigma_{12}^{(L)}(R_2^t)=\frac{2L+1}{2E+1}|S_{12}^{(0)}|^2. \tag{A13}$$

The modulus square of the S matrix in the absence of the TOB region, $|S_{12}^{(0)}|^2$, is computed according to Eqs. (12)–(14) and $|\mathcal{T}|^2$ is computed according to Eq. (A11). These equations are valid for energies both through and above the TOB. Note, when $E=\varepsilon_2'(R_T)$, $|\mathcal{R}|^2=|\mathcal{T}|^2=1/2$.

APPENDIX B: CORRECTION TERM TO THE HIDDEN-CROSSING METHOD

The one-Sturmian theory [27] can be used to correct the hidden-crossing method to take into account the factor $(\langle\varphi|d^2\varphi/dR^2\rangle+(1/4)/R^2)$. The factor $W_{\mu,\mu}=-\frac{1}{2}\langle\varphi_\mu|d^2\varphi_\mu/dR^2\rangle$ is the usual diagonal nonadiabatic correction to the adiabatic potential $\varepsilon_\mu(R)$. To show how it obtains from the one-Sturmian theory, a short derivation is presented in this appendix.

The one-Sturmian approximation for the wave function is

$$\Psi(R,\Omega)=\int_c\frac{1}{\rho(\nu)}B(\nu)S(\nu,\omega)R^{1/2}Z_\nu(KR)\,\nu d\nu, \tag{B1}$$

where c denotes a contour in the complex plane and the coefficient $B(\nu)$ satisfies the three-term recurrence relation:

$$\frac{2\nu}{K\rho(\nu)}B(\nu)=M(\nu)B(\nu+1)+M(\nu-1)B(\nu-1), \tag{B2}$$

where

$$\begin{aligned}M(\nu)&=-\int S(\nu+1;\Omega)2C(\Omega)S(\nu;\Omega)d\Omega\\&\equiv-\langle S(\nu+1)|2C|S(\nu)\rangle.\end{aligned} \tag{B3}$$

Note that the inner product of Sturmian basis functions is defined without the complex conjugate.

In the derivation of the hidden-crossing theory [27], a further approximation is made, namely, the matrix element Eq. (B3) is evaluated by expanding $S(\nu';\Omega)$, $\nu'=\nu\pm1$, about the point $\nu'=\nu$ and taking the lowest-order term only. The lowest-order term to $M(\nu)$ equals unity and the next-order term vanishes by the normalization condition Eq. (4). However, the second-order terms give rise to a correction to the hidden-crossing theory.

To compute this correction, note that the matrix element $M(\nu)$, to second-order is given by

$$M(\nu)\approx M(\nu-1)\approx\left(1+\frac{1}{2}\left\langle\frac{\partial^2 S}{\partial\nu^2}\right|-2C(\Omega)\left|S\right\rangle\right). \tag{B4}$$

Substituting Eq. (B4) in Eq. (B2) gives

$$\begin{aligned}\frac{2\nu}{K}A(\nu)=&\left(1+\frac{1}{2}\left\langle\frac{\partial^2 S}{\partial\nu^2}\right|-2C(\Omega)\left|S\right\rangle\right)[\rho(\nu+1)A(\nu+1)\\&+\rho(\nu-1)A(\nu-1)].\end{aligned} \tag{B5}$$

The one-Sturmian results of Ref. [27] can be taken over by defining

$$\rho_{\rm eff}(\nu)=\rho(\nu)\left(1+\frac{1}{2}\left\langle\frac{\partial^2 S}{\partial\nu^2}\right|-2C(\Omega)\left|S\right\rangle\right) \tag{B6}$$

and replacing $\rho(\nu)$ with $\rho_{\rm eff}(\nu)$ in the equations. Below we derive a general expression for $\langle\partial^2 S/\partial\nu^2|-2C(\Omega)|S\rangle$ and consider approximations to it when $\varepsilon(\rho)$ is a slowing varying function of ρ.

We begin with the one-Sturmian equation, Eq. (3), and take the first and second derivative of this equation with respect to ν. The first derivative equation is projected onto $\partial^2 S/\partial\nu^2$ and the second derivative equation is projected onto $\partial S/\partial\nu$. The difference of the resulting two equations gives

$$\begin{aligned}&\frac{\partial\rho}{\partial\nu}\left[\left\langle\frac{\partial^2 S}{\partial\nu^2}\right|2C(\Omega)\left|S\right\rangle-2\left\langle\frac{\partial S}{\partial\nu}\right|2C(\Omega)\left|\frac{\partial S}{\partial\nu}\right\rangle\right]-2\nu\left\langle\frac{\partial^2 S}{\partial\nu^2}\right|S\Big\rangle\\&\quad+4\nu\left\langle\frac{\partial S}{\partial\nu}\right|\frac{\partial S}{\partial\nu}\Big\rangle+2\left\langle\frac{\partial S}{\partial\nu}\right|S\Big\rangle=0,\end{aligned} \tag{B7}$$

where the normalization condition Eq. (4) has been used.

Using the identities,

$$\langle S|S\rangle=N^2=-\frac{1}{2\nu}\frac{\partial\rho}{\partial\nu}, \tag{B8}$$

$$\left\langle\frac{\partial S}{\partial\nu}\right|S\Big\rangle=\frac{1}{2}\frac{\partial N^2}{\partial\nu}, \tag{B9}$$

$$\left\langle\frac{\partial^2 S}{\partial\nu^2}\right|S\Big\rangle=-\left\langle\frac{\partial S}{\partial\nu}\right|\frac{\partial S}{\partial\nu}\Big\rangle+\frac{1}{2}\frac{\partial^2 N^2}{\partial\nu^2}, \tag{B10}$$

$$\left\langle\frac{\partial^2 S}{\partial\nu^2}\right|2C(\Omega)\left|S\right\rangle=-\left\langle\frac{\partial S}{\partial\nu}\right|2C(\Omega)\left|\frac{\partial S}{\partial\nu}\right\rangle, \tag{B11}$$

in Eq. (B7) gives

$$-N^2\left\langle\frac{\partial^2 S}{\partial\nu^2}\right|2C(\Omega)\left|S\right\rangle-\left\langle\frac{\partial^2 S}{\partial\nu^2}\right|S\Big\rangle+\frac{1}{3}\frac{\partial^2 N^2}{\partial\nu^2}+\frac{1}{6\nu}\frac{\partial N^2}{\partial\nu}=0. \tag{B12}$$

Because of the relation between the Sturmian and adiabatic functions, Eq. (6), we have

$$\left\langle \frac{\partial^2 S}{\partial \nu^2} \middle| S \right\rangle = N \frac{\partial^2 N}{\partial \nu^2} + N^2 \left\langle \frac{\partial^2 \varphi}{\partial \nu^2} \middle| \varphi \right\rangle. \tag{B13}$$

Using this equation together with

$$N \frac{\partial^2 N}{\partial \nu^2} = \frac{-1}{4N^2} \left(\frac{\partial N^2}{\partial \nu} \right)^2 + \frac{1}{2} \frac{\partial^2 N^2}{\partial \nu^2}, \tag{B14}$$

$$\left\langle \frac{\partial^2 \varphi}{\partial \nu^2} \middle| \varphi \right\rangle = \left\langle \frac{\partial^2 \varphi}{\partial \rho^2} \middle| \varphi \right\rangle \left(\frac{\partial \rho}{\partial \nu} \right)^2, \tag{B15}$$

in Eq. (B12) we obtain

$$-N^2 \left\langle \frac{\partial^2 S}{\partial \nu^2} \middle| 2C(\Omega) \middle| S \right\rangle = 4\nu^2 N^6 \left\langle \frac{\partial^2 \varphi}{\partial \rho^2} \middle| \varphi \right\rangle + \frac{1}{6} \frac{\partial^2 N^2}{\partial \nu^2} - \frac{1}{4N^2} \left(\frac{\partial N^2}{\partial \nu} \right)^2 - \frac{1}{6\nu} \frac{\partial N^2}{\partial \nu}. \tag{B16}$$

Now, using the normalization $N(\nu)$ given by Eq. (7) we obtain

$$N^2 = -\frac{\partial \rho}{2\nu \partial \nu} = -\frac{1/2}{\left[\frac{\partial \varepsilon}{\partial \rho} \rho^2 + 2\varepsilon\rho \right]} \tag{B17}$$

and

$$-\frac{\partial}{2\nu \partial \nu} = -\frac{1/2}{\left[\frac{\partial \varepsilon}{\partial \rho} \rho^2 + 2\varepsilon\rho \right]} \frac{\partial}{\partial \rho} = N^2 \frac{\partial}{\partial \rho}. \tag{B18}$$

These equations yield an alternative form of the second derivative term, namely,

$$\left\langle \frac{\partial^2 S}{\partial \nu^2} \middle| -2C(\Omega) \middle| S \right\rangle = 4\nu^2 N^4 \left\langle \frac{\partial^2 \varphi}{\partial \rho^2} \middle| \varphi \right\rangle + \nu^2 N^2 \frac{2}{3} \frac{\partial^2 N^2}{\partial \rho^2} - \nu^2 \frac{1}{3} \left(\frac{\partial N^2}{\partial \rho} \right)^2. \tag{B19}$$

Consider the case where $\varepsilon(\rho)$ is a slowly varying function of ρ is the sense that $\varepsilon'(\rho) \approx 0$. Then,

$$4\nu^2 N^4 \approx \frac{\nu^2}{4\varepsilon^2 \rho^2} = \frac{1}{2\varepsilon} \left(1 + \frac{1}{8\varepsilon\rho^2} \right), \tag{B20}$$

$$\nu^2 N^2 \frac{2}{3} \frac{\partial^2 N^2}{\partial \rho^2} \approx \frac{1}{12} \frac{\nu^2}{\varepsilon^2 \rho^4}, \tag{B21}$$

$$\nu^2 \frac{1}{3} \left(\frac{\partial N^2}{\partial \rho} \right)^2 \approx \frac{1}{48} \frac{\nu^2}{\varepsilon^2 \rho^4}. \tag{B22}$$

Substituting these equations into Eq. (B19) leads to

$$\left\langle \frac{\partial^2 S}{\partial \nu^2} \middle| -2C(\Omega) \middle| S \right\rangle \approx \frac{\nu^2}{4\varepsilon^2 \rho^2} \left(\left\langle \frac{\partial^2 \varphi}{\partial \rho^2} \middle| \varphi \right\rangle + \frac{1}{4\rho^2} \right) \approx \frac{1}{2\varepsilon} \left(1 + \frac{1}{8\varepsilon\rho^2} \right) \left(\left\langle \frac{\partial^2 \varphi}{\partial \rho^2} \middle| \varphi \right\rangle + \frac{1}{4\rho^2} \right). \tag{B23}$$

Replacing $\rho(\nu)$ by $\rho_{\text{eff}}(\nu)$ in Eq. (10) gives

$$K^2(\rho) \approx 2E - \frac{\nu^2}{\rho_{\text{eff}}^2} \approx 2E - \frac{\nu^2}{\rho^2 \left(1 + \frac{1}{2} \left\langle \frac{\partial^2 S}{\partial \nu^2} \middle| -2C(\Omega) \middle| S \right\rangle \right)^2}, \tag{B24}$$

$$\approx 2E - \frac{\nu^2}{\rho^2} \left(1 - \left\langle \frac{\partial^2 S}{\partial \nu^2} \middle| -2C(\Omega) \middle| S \right\rangle \right) \tag{B25}$$

$$\approx 2E - \frac{\nu^2}{\rho^2} + \frac{\nu^4}{4\varepsilon^2 \rho^4} \left(\left\langle \frac{\partial^2 \varphi}{\partial \rho^2} \middle| \varphi \right\rangle + \frac{1}{4\rho^2} \right). \tag{B26}$$

Using Eq. (5) in Eq. (B26) gives

$$K^2(\rho) = 2E - 2\varepsilon - 2W(\rho), \tag{B27}$$

where

$$W(\rho) = -\frac{1}{2} \left\langle \frac{\partial^2 \varphi}{\partial \rho^2} \middle| \varphi \right\rangle \tag{B28}$$

with the neglect of terms of order ρ^{-4}. Equation (B27) is appropriate for large ρ since there $\varepsilon(\rho)$ is a slowly varying function of ρ.

In Eq. (B26) the correction term to the hidden-crossing theory is $\langle \partial^2 \varphi / \partial \rho^2 | \varphi \rangle + 1/4\rho^2$, which includes the Langer correction $1/4\rho^2$. In the final equation for $K^2(\rho)$ the Langer correction subtracts out. Then the term $\varepsilon + W$ agrees with the close-coupling asymptotic channel potentials through terms of order $1/R^2$.

According to this discussion the diagonal nonadiabatic term should be used only when $\varepsilon(\rho)$ is a slowly varying function of ρ. For example when $\varepsilon(\rho) = a + b/\rho^2$, then the relation Eq. (B23) is seen to hold for sufficiently large ρ and $a \neq 0$. Alternatively, when $\varepsilon(\rho)$ has a branch point at R_b, then $\varepsilon'(R_b)$ is infinite and $W(R_b)$ diverges. At this point, however, the left-hand side of Eq. (B23) is finite. For this reason, $W(\rho)$ should not be employed near avoided crossing, but should be kept for large real ρ.

[1] W. Sperber, D. Becker, K. G. Lynn, W. Raith, A. Schwab, G. Sinapius, G. Spicher, and M. Weber, Phys. Rev. Lett. **68**, 3690 (1992).
[2] M. Weber, A. Holmann, W. Raith, W. Sperber, F. Jacobsen, and K. G. Lynn, Hyperfine Interact. **89**, 221 (1994).
[3] S. Zhou, H. Li, W. E. Kauppila, C. K. Kwan, and T. S. Stein, Phys. Rev. A **55**, 361 (1996).
[4] V. Kara, K. Paludan, J. Moxom, and G. Laricchia (unpublished).
[5] H. S. W. Massey, Can. J. Phys. **60**, 461 (1982).
[6] M. Leventhal and B. L. Brown, in *Proceedings of the Third International Workshop on Positron (Electron)-Gas Scattering*, edited by W. E. Kauppila, T. S. Stein, and J. Wadehra (World Scientific, Sinapore, 1986), p. 140.
[7] E. Stokstad, Science **276**, 897 (1997).
[8] H. S. W. Massey, Phys. Today **29** (3), 42 (1976).
[9] J. W. Humberston, M. Charlton, F. M. Jacobsen, and B. I. Deutch, J. Phys. B **20**, L25 (1987).
[10] J. W. Humberston, Can. J. Phys. **60**, 591 (1982).
[11] J. W. Humberston, J. Phys. B **17**, 2353 (1984).
[12] J. W. Humberston, Adv. At. Mol. Phys. **22**, 1 (1986).
[13] C. J. Brown and J. W. Humberston, J. Phys. B **17**, L423 (1984).
[14] J. W. Humberston, P. Van Reeth, M. S. T. Watts, and W. E. Meyerhof, J. Phys. B **30**, 2477 (1997).
[15] C. J. Brown and J. W. Humberston, J. Phys. B **18**, L401 (1985).
[16] M. T. McAlinden, A. A. Kernoghan, and H. R. J. Walters, Hyperfine Interact. **89**, 161 (1994).
[17] A. A. Kernoghan, M. T. McAlinden, and H. R. J. Walters, J. Phys. B **28**, 1079 (1995).
[18] A. A. Kernoghan, D. J. R. Robinson, M. T. McAlinden, and H. R. J. Walters, J. Phys. B **29**, 2089 (1996).
[19] J. Mitroy, L. Berge, and A. Stelbovics, Phys. Rev. Lett. **73**, 2966 (1994).
[20] J. Mitroy, Aust. J. Phys. **48**, 646 (1995).
[21] J. Mitroy, J. Phys. B **29**, L263 (1996).
[22] T. T. Gien, Phys. Rev. A **56**, 1332 (1997).
[23] A. Igarashi and N. Toshima, Phys. Rev. A **50**, 232 (1994).
[24] Y. Zhou and C. D. Lin, J. Phys. B **27**, 5065 (1994).
[25] Y. Zhou and C. D. Lin, J. Phys. B **28**, 4907 (1995).
[26] Y. Zhou and C. D. Lin, Can. J. Phys. **74**, 353 (1996).
[27] J. H. Macek and S. Yu. Ovchinnikov, Phys. Rev. A **54**, 544 (1996).
[28] S. J. Ward, J. H. Macek, and S. Yu. Ovchinnikov, in *Application of Accelerators in Research and Industry*: Proceedings of the Fourteenth International Conference, edited by J. L. Duggan and I. L. Morgan, AIP Conf. Proc. No. 392 (AIP, Woodbury, NY 1997), p. 469.
[29] S. J. Ward, J. H. Macek, and S. Yu. Ovchinnikov, Nucl. Instrum. Methods Phys. Res. B **143**, 175 (1998).
[30] R. K. Janev and E. A. Solov'ev, in *Photonic, Electronic, and Atomic Collisions, Invited Papers of the XX International Conference on the Physics of Electronic and Atomic Collisions, Vienna, Austria, 1997*, edited by F. Aumayr and H. Winter (World Scientific, Singapore, 1998), p. 393.
[31] J. H. Macek (unpublished).
[32] J. H. Macek, in *Application of Accelerators in Research and Industry*; Proceedings of the Fourteenth International Conference, (Ref. [28], p. 11.
[33] J. H. Macek, S. Yu. Ovchinnikov, and S. V. Pasovets, Phys. Rev. Lett. **74**, 4631 (1995).
[34] S. V. Passovets, J. H. Macek, and S. Yu. Ovchinnikov, in *The Physics of Electronic and Atomic Collisions*: XIX International Conference No. edited by L. J. Dubé, J. B. A. Mitchell, J. W. McKonkey, and C. E. Brion, AIP Conf. Proc. No. 360 (AIP, Woodbury, NY, 1995), p. 347.
[35] P. Ashley, J. Moxom, and G. Laricchia, Phys. Rev. Lett. **77**, 1250 (1996).
[36] W. Ihra, J. H. Macek, F. Mota-Furtado, and P. F. O'Mahony, Phys. Rev. Lett. **78**, 4027 (1997).
[37] L. D. Landau and E. M. Lifshitz, *Quantum Mechanics: Non-Relativistic Theory* (Pergamon Press, Oxford, 1981), Chap. 7, p. 164ff.
[38] A. Erdelyi, W. Magnus, F. Oberhettinger, and F. G. Triocomi, *Higher Transcendental Functions* (McGraw-Hill, New York, 1953), Vol. II, p. 75.
[39] T. H. Gronwall, Ann. Math. **33**, 279 (1932).
[40] J. Macek, J. Phys. B **1**, 831 (1968).
[41] Yu. Demkov, in *The Physics of Electronic and Atomic Collisions, Leningrad, 1967*, Proceedings of Invited Papers of the XI International Conference, edited by I. P. Flaks and E. A. Solov'ev (Joint Institute for Laboratory Astrophysics, Boulder, CO, 1968), p. 186.
[42] U. Fano and A. R. P. Rau, *Atomic Collisions and Spectra* (Academic Press, Orlando, FL, 1986), p. 153ff.
[43] E. E. Nikitin and S. Yu. Umanskii, *Theory of Slow Atomic Collisions* (Springer-Verlag, Berlin, 1984).
[44] C. Bottcher, Adv. At. Mol. Phys. **25**, 303 (1989).
[45] A. S. Umar, J. Wu, M. R. Strayer, and C. Bottcher, J. Comput. Phys. **93**, 426 (1991).
[46] J. Wells, V. E. Oberacker, A. S. Umar, C. Bottcher, M. R. Strayer, J. S. Wu, and G. Plunier, Phys. Rev. A **45**, 6296 (1992).
[47] D. R. Kegley, Jr., V. E. Oberacker, M. R. Strayer, A. S. Umar, and J. C. Wells, J. Comput. Phys. **128**, 197 (1996).
[48] E. Anderson, Z. Bai, C. Bischof, J. Demmel, J. Dongarra, J. Du Croz, A. Greenbaum, S. Hammarling, A. McKenney, S. Ostrouchov, and D. Sorensen, *LAPACK User's Guide*, 2nd ed. (Society for Industrial and Applied Mathematics, Philadelphia, 1995), p. 179.
[49] J. W. Humberston and P. Van Reeth (private communication).
[50] G. Laricchia, Nucl. Instrum. Methods Phys. Res. B **99**, 363 (1995).
[51] J. H. Macek and S. Yu. Ovchinnikov, Phys. Rev. A **50**, 468 (1994).
[52] Z. Zhen and J. Macek, Phys. Rev. A **34**, 838 (1986).
[53] M. Cavagnero, Z. Zhen, and J. Macek, Phys. Rev. A **41**, 1225 (1990).
[54] *Handbook of Mathematical Functions*, edited by Milton Abramowitz and Irene A. Stegun (Dover, New York, 1972).